

Size properties of the largest fragments produced in the framework of the statistical multifragmentation model

S.R. Souza^{1,2} and R. Donangelo^{1,3}

¹*Instituto de Física, Universidade Federal do Rio de Janeiro Cidade Universitária,
Caixa Postal 68528, 21941-972 Rio de Janeiro-RJ, Brazil*

²*Departamento de Física, ICEx, Universidade Federal de Minas Gerais,
Av. Antônio Carlos, 6627, 31270-901 Belo Horizonte-MG, Brazil*

³*Instituto de Física, Facultad de Ingeniería, Universidad de la República,
Julio Herrera y Reissig 565, 11.300 Montevideo, Uruguay*

(Dated: April 28, 2020)

We study the size properties of the largest intermediate mass fragments in each partition mode, produced in the prompt statistical breakup of a thermally equilibrated nuclear source, at different temperatures. We find that an appreciable amount of events have primary intermediate mass fragments of similar sizes. Our results suggest that, depending on the temperature of the fragmenting source, their production may be much larger than what would be expected from considerations based on purely combinatorial arrangements of the nucleons in the fragmenting system. We also find that the isospin composition of the largest fragments is sensitive to their rank size within the event. We suggest that experimental analyses, conceived to reconstruct the breakup configuration, should be employed to investigate the validity of our findings.

PACS numbers: 25.70.Pq, 24.60.-k

I. INTRODUCTION

The understanding of the dynamics of the violent collision of two heavy ions at bombarding energies ranging from a few tens to a few hundreds MeV per nucleon, leading to many nuclear fragments in the exit channel, has been a challenge for both theorists and experimentalists during the last few decades [1–5]. Although a copious production of complex fragments in central and mid-central collisions has been clearly established, the mechanisms leading to it have been interpreted in different scenarios. Indeed, many properties of the fragments observed experimentally have been explained by statistical models [1, 2, 6–8], whereas many features are also adequately described by dynamical treatments, which range from classical and semi-classical formulations [5, 9, 10] to quantum approaches [11, 12]. Hybrid treatments have also been employed to match different different stages of the reaction, so that one approach provides the input information to the other [3, 13, 14] or act concomitantly [15], merging different mechanisms.

Among the different predictions made by the dynamical models, the emergence of regions of negative compressibility of the nuclear matter, *i.e.* regions of spinodal instability, allows the development of instabilities that would lead to the breakup of the system [16–19]. A salient feature of this mechanism is the formation of nearly sized fragments [3, 4, 16–20]. The detection of such events has challenged experimentalists since different factors make it very difficult to draw precise conclusions on this respect. For instance, the deexcitation of these fragments after the breakup could obscure their resemblance when they were formed. Experimental indications of the existence of such events have been reported recently [20] and the discussion on whether they are due

to merely combinatorial arrangements of a finite number of nucleons, or are actually due to the development of spinodal instabilities, has been addressed based on correlations proposed in Ref. [21].

In this work, we examine the properties of the largest fragments formed in the prompt statistical breakup of a nuclear source in thermal equilibrium. We investigate whether the production of similar sized fragments is dominated by combinatorial arrangements of nucleons or by the statistical weights associated with the accessible phase space. In order to eliminate difficulties associated with the incomplete sampling of the huge partition space, we use a version of the Statistical Multifragmentation Model (SMM) [22–24] based on the exact recurrence formulae developed in Refs. [25, 26]. Focusing on partitions with only a few large fragments, the equations derived in this work allow the calculation of the individual properties of each of these partitions. The manuscript is organized as follows. The main features of the SMM are recalled in Sect. II, where the formulae used in this work are derived. The results are presented in Sect. III and the main conclusions are drawn in Sect. IV.

II. THEORETICAL FRAMEWORK

The SMM is described in detail in the original works where it has been formulated [22–24]. Modifications to include improved binding energies and internal Helmholtz free energies are also carefully discussed in refs. [27, 28]. Therefore, in subsect. II A, we briefly sketch the main points useful in the discussion below and focus, in subsect. II B, on the derivation of the formulae employed in our analysis.

It is assumed that a thermal equilibrated source of

mass and atomic numbers A_0 and Z_0 , respectively, is formed at temperature T and density ρ and that it undergoes a prompt statistical breakup. As in previous studies [28], we adopt $\rho = \rho_0/6$, where ρ_0 corresponds to the normal nuclear matter density. In order to examine the sensitivity of the results to the excitation of the system, different values of the breakup temperature are used in Sect. III.

A. The SMM

Partitions are generated according to mass and charge conservation, so that the multiplicities $\{n_i\}$ of fragments of mass and atomic numbers a_i and z_i , respectively, are subject to the constraints:

$$\sum_i n_i a_i = A_0 \quad \text{and} \quad \sum_i n_i z_i = Z_0. \quad (1)$$

In the canonical formulation of the model [29], the statistical weight associated with a fragmentation mode $f = \{(a_1, z_1) \cdots (a_m, z_m)\}$, $m \equiv \sum_i n_i$, fulfilling the above constraints, is given by the partition function:

$$\Omega_f = \exp \left[-\frac{F_f(T, V)}{T} \right], \quad (2)$$

where V corresponds to the breakup volume and $F_f(T, V)$ symbolizes the Helmholtz free energy associated with the fragmentation mode [28, 29].

As discussed in Ref. [24], the number of different partitions rapidly becomes prohibitively large to allow the direct generation of all of them. For this reason, the standard SMM adopts a Monte Carlo strategy, in which different fragmentation modes are generated based on the combinatorial weight W_f^{-1} of a partition f [24]. In this way, the average value of an observable O , associated with the primary hot fragments, is given by:

$$\langle O \rangle = \frac{\sum_f O_f \Omega_f W_f}{\sum_f \Omega_f W_f}. \quad (3)$$

Since most of the primary fragments are very excited, their yields will be significantly affected in most cases [15, 28, 30, 31]. However, as we are interested in the system's properties at the point it disassembles, we will not consider their deexcitation.

It should be stressed that the combinatorial factor which appears in the above equation is meant to correct for the fact that the partitions $\{f\}$, which enter into Eq. (3), are not generated by the Monte Carlo sampling with equal probability. Rather, they are selected according to a distribution W_f^{-1} [24]. Therefore, the average value of an observable, calculated considering only the possible combinatorial arrangements of $A_0 - Z_0$ neutrons and Z_0

protons, assuming that they occur with equal probability, *i.e.* disregarding all other physical effects, is given by:

$$\langle \tilde{O} \rangle = \frac{\sum_f O_f W_f}{\sum_f W_f}. \quad (4)$$

In order to evaluate the enhancement or suppression of $\langle O \rangle$ with respect to what would be obtained considering only constraints due to this combinatorial arrangement, one may calculate the ratio:

$$R_O = \frac{\langle O \rangle}{\langle \tilde{O} \rangle}. \quad (5)$$

However, owing to the huge number of partitions in the case of systems of actual interest, average values of observables may be subject to large fluctuations, if their main contributions arise from rare events. Thus, ratios based on such observables may be significantly affected by the rather reduced sampling of the configurations. This assertion remains valid even if a very large (but practically feasible) number of partitions is generated, as they would consider only a very small fraction of the total set. This is particularly important if the denominator of the ratio is small. We have checked that this indeed happens in the case of the observables discussed in the next section, even if as many as 10^9 Monte Carlo partitions are sampled.

B. Recurrence relations

To eliminate this difficulty, we resort to the formulation developed by Das Gupta and Mekjian [25, 26], in which different observables may be exactly calculated through recurrence relations. More specifically, the statistical weight associated with a source (A_0, Z_0) is written as:

$$\Omega_{A_0, Z_0} = \sum_{f \in F_0} \prod_{i \in f} \frac{\omega_i^{n_i}}{n_i!}, \quad (6)$$

where F_0 symbolizes the set of partitions consistent with the constraints expressed by Eq. (1) and

$$\omega_i = \left(\frac{g_i V_f}{\lambda_T^3} A_i^{3/2} \right) \exp(-\mathcal{F}_i/T). \quad (7)$$

In the above equation, g_i denotes the spin degeneracy factor of the species (a_i, z_i) , $\lambda_T = \sqrt{2\pi\hbar^2/mT}$, m is the nucleon mass and \mathcal{F}_i symbolizes the contribution of species i to the total Helmholtz free energy. It contains terms associated with its binding energy and to the Wigner-Seitz

corrections to the Coulomb energy [22], besides others associated with its internal excitation [32].

Das Gupta and Mekjian [25, 26] realized that very efficient recursion relations could be obtained from Eq. (6) and derived the following result:

$$\Omega_{A_0, Z_0} = \sum_{(a_i, z_i) \in S_0} \frac{a_i}{A_0} \omega_i \Omega_{A_0 - a_i, Z_0 - z_i}, \quad (8)$$

where S_0 corresponds to the set composed of all species $\{(a_i, z_i)\}$ for which $(a_i, z_i) \leq (A_0, Z_0)$.

In the same vein, we extend this idea to calculate the probability of observing a particular partition $f \in F_0$, which contains a subset $s = \{n_1, \dots, n_{m_0}\}$ of $M = \sum_{i=1}^{m_0} n_i$ fragments, $s \subset f$, which fulfills a condition \mathcal{C} :

$$\tilde{P}_{s,f} = \frac{1}{\Omega_{A_0, Z_0}} \left(\prod_{i \in s} \frac{\omega_i^{n_i}}{n_i!} \right) \left(\prod_{k \in f \setminus s} \frac{\omega_k^{n_k}}{n_k!} \right). \quad (9)$$

We denote the subset made up of these particular partitions f by $F_{0,s}$. By defining

$$\Omega_s^* \equiv \prod_{i \in s} \frac{\omega_i^{n_i}}{n_i!}, \quad (10)$$

$$\tilde{\Omega}_{A_0, Z_0}^s \equiv \sum_{f \in F_{0,s}} \prod_{k \in f \setminus s} \frac{\omega_k^{n_k}}{n_k!}, \quad (11)$$

the probability of observing the set of fragments s among all possible partitions is given by:

$$P_s = \sum_{f \in F_{0,s}} \tilde{P}_{s,f} = \frac{1}{\Omega_{A_0, Z_0}} \Omega_s^* \tilde{\Omega}_{A_0, Z_0}^s. \quad (12)$$

If M is small and the fragmenting source is not too large, the above equations can be evaluated numerically, considering all the possible partitions, if the condition \mathcal{C} is strict enough. For instance, considering $A_0 = 189$, $Z_0 = 83$ (which in our implementation of the SMM gives 3209 species in set S_0), fragmentation modes containing only M fragments with $z \geq 5$, the subsets s with $M = 3$ and 4 such fragments have 2.43961×10^8 and 1.62527×10^{10} partitions, respectively. Although the evaluation of observables associated with the selected fragments within these partitions is time consuming, it is a feasible task using the present computational resources. One should note that the partitions which are actually calculated individually are the subsets s , entering into Eq. (12), *i.e.* Ω_s^* . The remaining contribution is taken into account by $\tilde{\Omega}_{A_0, Z_0}^s$, which is evaluated recursively through Eq. (8), including only species which are not in s . Otherwise, the number of partitions would be too large to allow the direct evaluation of the sums which enter into the above expressions, even in the rather particular cases exemplified above.

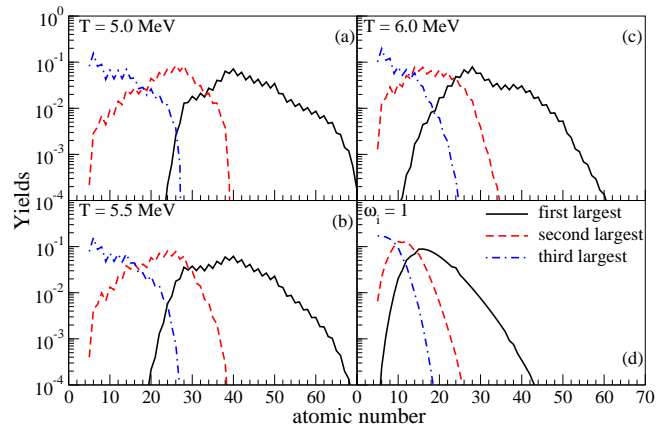


FIG. 1. (Color online) Charge distribution of the first, second, and third, largest fragments in events in which $M = 3$ fragments have atomic number $z \geq 5$, for different breakup temperatures, panels (a)-(c). In panel (d) the fragments appear in the partitions according to rules dictated by the combinatorial arrangements of $A_0 - Z_0$ neutrons and Z_0 protons. For details, see the text.

III. RESULTS

We now apply the model to study some properties of the fragments produced in the fragmentation of a source of size $A_0 = 189$ and $Z_0 = 83$. As in the calculations reported in Ref. [20], this corresponds to 80% of the $^{124}\text{Xe} + ^{112}\text{Sn}$ system, studied experimentally in that work.

We start by considering the charge distribution of the fragments observed in partitions $f \in F_{0,s}$ which fulfill the condition \mathcal{C} that the M largest fragments have atomic numbers $z \geq 5$, whereas the others have smaller atomic numbers. We calculate the average yields of the k -th largest fragments using P_s , given by Eq. (12):

$$\langle Y_k(z) \rangle = \left(\sum_{\substack{s \in S_M^* \\ z_k \in s}} P_s \delta_{z, z_k} \right) / \left(\sum_{s \in S_M} P_s \right), \quad (13)$$

where S_M^* denotes the subset of fragments within the partitions fulfilling the condition \mathcal{C} and δ is the Kronecker delta.

This is displayed in panels (a)-(c) in Fig. 1 for $M = 3$ and breakup temperatures $T = 5.0, 5.5,$ and 6.0 MeV. One sees that, as the temperature rises, the distributions of the first, second, and third largest fragments become narrower and their peaks shift towards small z values, while the separation between them diminishes. The large separation between the peaks indicates that the fragment sizes are appreciably different in most cases. However, the overlap between the distributions suggests that there are partitions in which the 3 fragments have similar atomic numbers. Analogous conclusions hold for $M = 4$. These properties are in qualitative agreement

with the experimental findings reported in Ref. [20], but our results cannot be directly compared to those data as we focus on the system's configuration at the breakup stage and do not consider the subsequent deexcitation of the fragments.

The nonvanishing overlap between the distributions displayed in panels (a)-(c) of Fig. 1 shows that large fragments of similar sizes may also be produced in the statistical breakup of the system. Hence, the existence of events with this property is not an exclusive feature of the disassembly by spinodal instabilities, predicted by dynamical mean field calculations [16–19]. However, there still remains the question of whether the existence of such events in statistical multifragmentation merely reflects the constraints associated with the mass/charge conservation laws and the combinatorial arrangements of the nucleons. To examine this point, we show in panel (d) the charge distribution of the M fragments obtained assuming $\omega_i = 1$ in Eqs. (9)-(11). In this way, the fragments contribute the same weight to the partition, except for the factors $(n_i!)^{-1}$ associated with the proper counting of identical fragments. This is also adopted in different methods used to generate partitions [7, 24]. One sees that the qualitative features observed in panels (a)-(c), considering the full statistical weight, are also present in this scenario and that the shape of the distributions is similar in both cases. However, the distributions shown in panel (d) are temperature independent. They are determined by the system size and the species included in the set S_0 . The distributions tend to become more and more similar to the full statistical ones as the temperature increases and the latter distributions shift to lower z values.

As in Ref. [20], we now consider the first and the second moments of the charge distribution of these M fragments in the subset s :

$$\langle z \rangle_s = \frac{1}{M} \sum_{i \in s} z_i \quad (14)$$

and

$$\sigma_{z,s} = \left[\frac{1}{M} \sum_{i \in s} (z_i - \langle z \rangle)^2 \right]^{1/2}. \quad (15)$$

From them, and using Eq. (12), we build the frequency with which sets of M fragments are observed with average value $\langle z \rangle$ and variance σ_z :

$$Y(\langle z \rangle, \sigma_z) = \left(\sum_{s \in S_M^*} P_s \Delta_{\langle z \rangle_s, \sigma_{z,s}} \right) / \left(\sum_{s \in S_M} P_s \right) \quad (16)$$

where

$$\Delta_{\langle z \rangle_s, \sigma_{z,s}} = \begin{cases} 1, & \text{if } \delta_{z,s} \leq \delta_z/2 \text{ and } \delta_{\sigma_{z,s}} \leq \delta_{\sigma_z}/2 \\ 0, & \text{otherwise,} \end{cases} \quad (17)$$

$\delta_{z,s} = | \langle z \rangle - \langle z \rangle_s |$, $\delta_{\sigma_{z,s}} = | \sigma_z - \sigma_{z,s} |$, and δ_z (δ_{σ_z}) is the bin size in the $\langle z \rangle$ (σ_z) axis.

This quantity is displayed in panels (a)-(c) of Fig. 2 (normalized to the largest value in each panel) for $M = 3$ and the different temperatures considered in this work. These results show that the distribution is peaked at large $\langle z \rangle$ values at the lowest temperature and the position of the bump moves to lower values as the temperature rises. The distribution is very broad along the σ_z axis, but it becomes narrower as the system is heated up. The position of the peak also moves to lower values as the temperature rises from $T = 5.5$ MeV to 6.0 MeV. At $T = 5.0$ MeV one observes two bumps along the σ_z axis which can be explained by the presence of one (two) large fragment(s) and two (one) smaller one (ones) in some events, whereas there are others in which the three fragments tend to be more similar. These bumps merge as T increases. It is important to note that there are no statistical fluctuations in these results, since the formulae derived in this work are exact within the framework of the model. Therefore, the patterns observed in the distributions are not artificial.

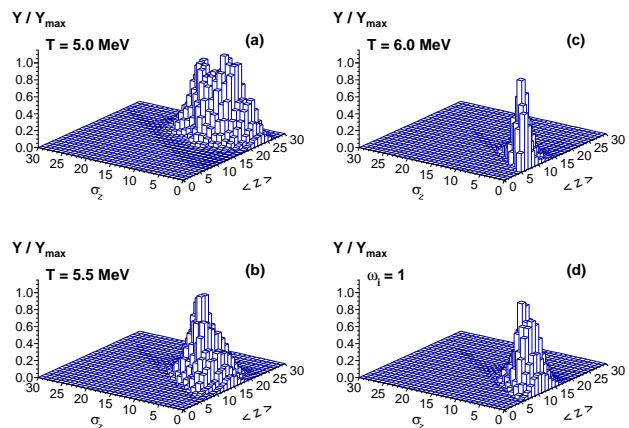


FIG. 2. (Color online) Panels (a)-(c): Distribution of partitions in which the $M = 3$ largest fragments (with atomic number $z \geq 5$) have average value $\langle z \rangle$ and standard deviation σ_z , for different breakup temperatures. Panel (d): The partitions are constructed considering only combinatorial arrangements of $A_0 - Z_0$ neutrons and Z_0 protons. For details, see the text.

Panel (d) of Fig. 2 shows the distribution $Y(\langle z \rangle, \sigma_z)$ obtained assuming $\omega_i = 1$. In this case, it is narrower than those obtained at $T \leq 5.5$ MeV and it is peaked at lower $\langle z \rangle$ and σ_z values. It is more similar to the distribution at $T = 6.0$ MeV. This shows that the statistical weights associated with the phase space available to the

partitions lead to very important deviations from the scenario of fragments populating the partitions according to combinatorial arrangements only.

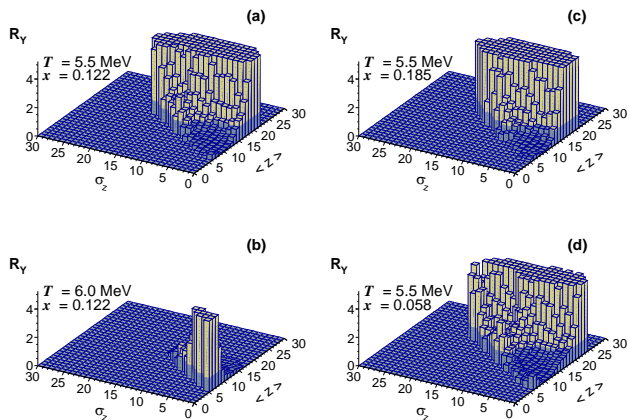


FIG. 3. (Color online) Ratio between the distribution $Y(\langle z \rangle, \sigma_z)$ calculated using the full statistical weight and the one obtained considering only the combinatorial arrangements of the nucleons, at different temperatures and asymmetry parameter $x = 1 - 2Z_0/A_0$ of the source of mass number $A_0 = 189$. For details, see the text.

For the purpose of providing a more quantitative interpretation of this aspect, Fig. 3 displays the ratio R_Y between $Y(\langle z \rangle, \sigma_z)$ calculated with the full statistical weight and the one obtained assuming $\omega_i = 1$, $Y(\langle z \rangle, \sigma_z, \omega_i = 1)$, in different cases. In order to eliminate contributions from events that are not representative, we only show the ratios if $Y(\langle z \rangle, \sigma_z) \geq 10^{-4}$. We also limit the vertical scale to $R_Y \leq 5$, since very large ratios are obtained if $Y(\langle z \rangle, \sigma_z, \omega_i = 1)$ is very small. This is the reason why the distributions look flat in some regions. Thus, we restrict the analysis to the regions where there is a competition between the constraints imposed by the combinatorial arrangements of the nucleons and the weights associated with the phase space available to the system.

Since at $T = 5.0$ MeV, $Y(\langle z \rangle, \sigma_z)$ is non-negligible only where $Y(\langle z \rangle, \sigma_z, \omega_i = 1)$ is very small, the results at this temperature are not shown in Fig. 3 and we focus on the highest two temperatures. In this plot, the blue (dark gray) areas correspond to $R_Y \leq 1$ whereas the light brown (light gray) ones are associated with $R_Y > 1$. In panels (a) and (b), we exhibit R_Y for $T = 5.5$ MeV and $T = 6.0$ MeV, respectively. In the former case, $R_Y < 1$ for $\langle z \rangle \lesssim 15$, except for $\sigma_z \gtrsim 10$. This indicates that the statistical weight of these configurations is not large enough to dominate the constraints associated with the combinatorial arrangements. The larger phase space available to configurations which give $\langle z \rangle \gtrsim 15$ tips the balance in its favor and one observes a rapid rise of R_Y in this region. The fact that $R_Y > 1$ also for very small values of σ_z , at non-negligible values of $Y(\langle z \rangle, \sigma_z)$, reveals that many partition modes with fragments of sim-

ilar sizes contribute to the distribution. Analogous conclusions also hold for different sources' isospin composition as one sees in panels (c) and (d) which show R_Y for sources, at $T = 5.5$ MeV, with $A_0 = 189$ and $x = 0.185$ and $x = 0.058$, respectively, where $x = 1 - 2Z_0/A_0$. The situation is very different at $T = 6.0$ MeV. The overlap between $Y(\langle z \rangle, \sigma_z)$ and $Y(\langle z \rangle, \sigma_z, \omega_i = 1)$ is appreciable and $R_Y \gg 1$ in most of the overlapping region. This is particularly pronounced at small σ_z . Thus, the existence of these very similar fragments is due to statistical considerations rather than to combinatorial constraints. Our results indicate that this dominance of the statistical weights over the combinatorial arrangements is sensitive

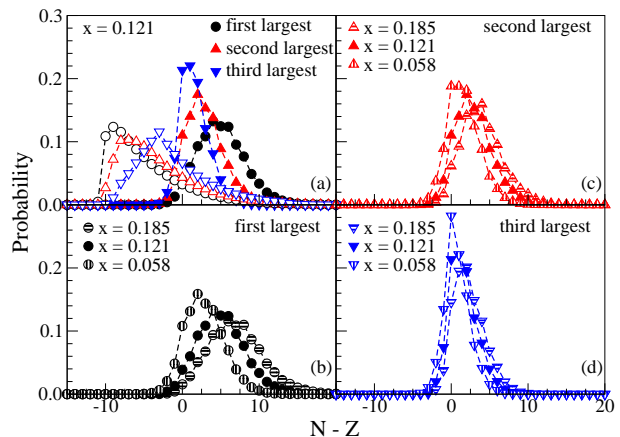


FIG. 4. (Color online) Distribution of the neutron-proton asymmetry of the largest three fragments for different values of the sources' asymmetry, at breakup temperature $T = 5.5$ MeV. The open symbols in frame (a) represent the results obtained with $\omega_i = 1$. For details, see the text.

Very different qualitative characteristics of the isospin composition of the largest fragments are observed whether one assumes that the fragmentation modes are ruled by combinatorial arrangements only, or takes into account the full statistical weights. This is illustrated in panel (a) of Fig. 4 which displays the $N - Z$ distribution of the $M = 3$ largest fragments, produced at $T = 5.5$ MeV, where N denotes the neutron number. It reveals that the isospin properties of the Helmholtz free energy leads to neutron richer fragments than considerations based only on combinatorial arrangements. It also shows that, in the former case, the largest fragments tend to be more neutron rich than the lighter ones. This reflects the tendency of nuclei of having equal number of neutrons and protons as their sizes diminish. Panels (b)-(c) of this figure compare the distributions for sources of different isospin compositions, for $A_0 = 189$, at $T = 5.5$ MeV. They show that the sensitivity to the isospin composition of the source weakens as the fragments' rank size decreases.

Finally, to investigate the influence of the breakup temperature on the $N - Z$ distribution of these largest frag-

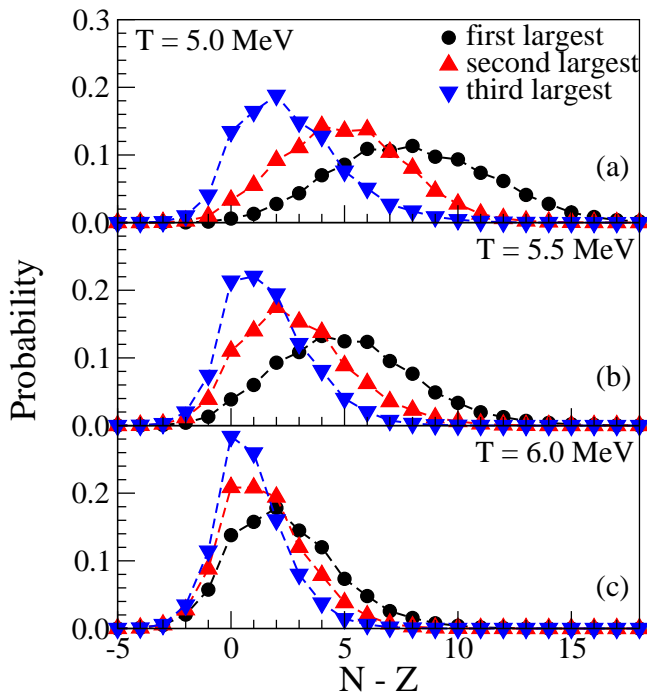


FIG. 5. (Color online) Same as Fig. 4 for $x = 0.121$ and different temperatures. For details, see the text.

ments, this quantity is exhibited in panels (a)-(c) of Fig. 5 at different temperatures. The results reveal that the distributions become narrower as T increases and the peaks move towards $N \approx Z$. Thus, they may help investigate the asymmetry energy term in the equation of state of the source at the breakup stage.

IV. CONCLUDING REMARKS

In the framework of the prompt statistical breakup of a nuclear source in thermal equilibrium at temperature T , we examined the properties of the largest M fragments produced in each fragmentation mode. We addressed the question of whether the production of many similar fragments within an event is ruled by combinatorial constraints or by statistical considerations. To this end, we employed a version of the SMM, presented in Refs.

[25, 26], based on recurrence formulae for the statistical weights, and derived expressions which allowed the individual calculation of each partition with M fragments of atomic number $z \geq z_{\min}$. Our results suggest that either aspect dominates certain configurations and that the balance between them is sensitive to the breakup temperature. More specifically, larger temperatures lead to larger phase space volumes accessible to the system and, therefore, tip the balance in favor of the statistical emission and one observes many fragments of similar sizes. However, we found that the partition mode also plays an important role as, for a given breakup temperature, the combinatorial arrangements of the nucleons dominate in certain configurations, which have access to smaller phase space volumes. We therefore suggest these properties should be further experimentally investigated, and that the configuration at the breakup be reconstructed as in Refs. [33–38]. Our results also suggest that the neutron-proton asymmetry of the M largest fragments is sensitive to their rank size and that this sensitivity weakens as the breakup temperature increases. The neutron-proton asymmetry of the source is also found to affect this property of the M largest fragments.

ACKNOWLEDGMENTS

This work was supported in part by the Brazilian agencies Conselho Nacional de Desenvolvimento Científico e Tecnológico (CNPq), by the Fundação Carlos Chagas Filho de Amparo à Pesquisa do Estado do Rio de Janeiro (FAPERJ), a BBP grant from the latter. We also thank the Uruguayan agencies Programa de Desarrollo de las Ciencias Básicas (PEDECIBA) and the Agencia Nacional de Investigación e Innovación (ANII) for partial financial support. This work has been done as a part of the project INCT-FNA, Proc. No.464898/2014-5. We also thank the Núcleo Avançado de Computação de Alto Desempenho (NACAD), Instituto Alberto Luiz Coimbra de Pós-Graduação e Pesquisa em Engenharia (COPPE), Universidade Federal do Rio de Janeiro (UFRJ), for the use of the supercomputer Lobo Carneiro, as well as the Cloud Veneto, where the calculations have been carried out.

-
- [1] L. G. Moretto and G. J. Wozniak, *Annu. Rev. Nucl. Part. Sci.* **43**, 379 (1993).
 - [2] S. Das Gupta, A. Z. Mekjian, and M. B. Tsang, *Adv. Nucl. Phys.* **26**, 89 (2001).
 - [3] B. Borderie and M. F. Rivet, *Prog. Part. Nucl. Phys.* **61**, 551 (2008).
 - [4] B. Borderie and J. Frankland, *Prog. Part. Nucl. Phys.* **105**, 82 (2019).
 - [5] Bao-An. Li, Lie-Wen. Chen, and Che Ming. Ko, *Phys. Rep.* **464**, 113 (2008).
 - [6] J. P. Bondorf, A. S. Botvina, A. S. Iljinov, I. N. Mihustin, and K. Sneppen, *Phys. Rep.* **257**, 133 (1995).
 - [7] D. Gross, *Phys. Rep.* **279**, 119 (1997).
 - [8] C. B. Das, S. Das Gupta, W. G. Lynch, A. Z. Mekjian, and M. B. Tsang, *Phys. Rep.* **406**, 1 (2005).
 - [9] J. Aichelin, *Phys. Rep.* **202**, 233 (1991).
 - [10] A. Bonasera, F. Gulminelli, and J. Molitoris, *Physics Reports* **243**, 1 (1994).
 - [11] H. Feldmeier and J. Schnack, *Prog. Part. Nucl. Phys.* **39**, 393 (1997).

- [12] A. Ono and H. Horiuchi, *Progress in Particle and Nuclear Physics* **53**, 501 (2004).
- [13] A. S. Botvina and I. N. Mishustin, *Eur. Phys. J. A* **30**, 121 (2006).
- [14] T. X. Liu, W. G. Lynch, M. J. van Goethem, X. D. Liu, R. Shomin, W. P. Tan, M. B. Tsang, G. Verde, A. Wagner, H. F. Xi, H. S. Xu, W. A. Friedman, S. R. Souza, R. Donangelo, L. Beaulieu, B. Davin, Y. Larochele, T. Lefort, R. T. de Souza, R. Yanez, V. E. Viola, R. J. Charity, and L. G. Sobotka, *Europhys. Lett.* **74**, 806 (2006).
- [15] S. Souza, B. Carlson, and R. Donangelo, *Nucl. Phys. A* **989**, 69 (2019).
- [16] G. F. Burgio, M. Baldo, and A. Rapisarda, *Physics Letters B* **321**, 307 (1994).
- [17] M. Baldo, G. F. Burgio, and A. Rapisarda, *Phys. Rev. C* **51**, 198 (1995).
- [18] M. Colonna, P. Chomaz, A. Guarnera, and B. Jacquot, *Phys. Rev. C* **51**, 2671 (1995).
- [19] M. Colonna, P. Chomaz, and A. Guarnera, *Nucl. Phys. A* **613**, 165 (1997).
- [20] B. Borderie, N. L. Neindre], M. Rivet, P. Dsesquelles, E. Bonnet, R. Bougault, A. Chbihi, D. Dell'Aquila, Q. Fable, J. Frankland, E. Galichet, D. Gruyer, D. Guinet, M. L. Commaraj], I. Lombardo, O. Lopez, L. Manduci, P. Napolitani, M. Prlog, E. Rosato, R. Roy, P. St-Onge, G. Verde, E. Vient, M. Vigilante, and J. Wieleczko, *Phys. Lett. B* **782**, 291 (2018).
- [21] P. Dsesquelles, *Phys. Rev. C* **65**, 034604 (2002).
- [22] J. P. Bondorf, R. Donangelo, I. N. Mishustin, C. Pethick, H. Schulz, and K. Sneppen, *Nucl. Phys.* **A443**, 321 (1985).
- [23] J. P. Bondorf, R. Donangelo, I. N. Mishustin, and H. Schulz, *Nucl. Phys.* **A444**, 460 (1985).
- [24] K. Sneppen, *Nucl. Phys.* **A470**, 213 (1987).
- [25] K. C. Chase and A. Z. Mekjian, *Phys. Rev. C* **52**, R2339 (1995).
- [26] S. Das Gupta and A. Z. Mekjian, *Phys. Rev. C* **57**, 1361 (1998).
- [27] S. R. Souza, P. Danielewicz, S. Das Gupta, R. Donangelo, W. A. Friedman, W. G. Lynch, W. P. Tan, and M. B. Tsang, *Phys. Rev. C* **67**, 051602(R) (2003).
- [28] W. P. Tan, S. R. Souza, R. J. Charity, R. Donangelo, W. G. Lynch, and M. B. Tsang, *Phys. Rev. C* **68**, 034609 (2003).
- [29] C. E. Aguiar, R. Donangelo, and S. R. Souza, *Phys. Rev. C* **73**, 024613 (2006).
- [30] S. R. Souza, B. V. Carlson, R. Donangelo, W. G. Lynch, and M. B. Tsang, *Phys. Rev. C* **88**, 014607 (2013).
- [31] S. R. Souza, R. Donangelo, W. G. Lynch, and M. B. Tsang, *Phys. Rev. C* **97**, 034614 (2018).
- [32] S. R. Souza, M. B. Tsang, R. Donangelo, W. G. Lynch, and A. W. Steiner, *Phys. Rev. C* **78**, 014605 (2008).
- [33] S. Piantelli, B. Borderie, E. Bonnet, N. L. Neindre, A. Raduta, M. Rivet, R. Bougault, A. Chbihi, R. Dayras, J. Frankland, E. Galichet, F. Gagnon-Moisan, D. Guinet, P. Lantesse, G. Lehaut, O. Lopez, D. Mercier, J. Moisan, M. Prlog, E. Rosato, R. Roy, B. Tamain, E. Vient, M. Vigilante, and J. Wieleczko, *Nuclear Physics A* **809**, 111 (2008).
- [34] S. Hudan, A. Chbihi, J. D. Frankland, A. Mignon, J. P. Wieleczko, G. Auger, N. Bellaize, B. Borderie, A. Botvina, R. Bougault, B. Bouriquet, A. M. Buta, J. Colin, D. Cussol, R. Dayras, D. Durand, E. Galichet, D. Guinet, B. Guiot, G. Lanzalone, Lantesse, F. Lavaud, Lecolley, R. Legrain, L. Neindre, O. Lopez, L. Manduci, J. Marie, L. Nalpas, J. Normand, M. Párlog, P. Pawłowski, M. Pichon, E. Plagnol, M. F. Rivet, E. Rosato, R. Roy, J. Steckmeyer, G. Tăbăcaru, B. Tamain, A. van Lauwe, E. Vient, M. Vigilante, and C. Volant (INDRA Collaboration), *Phys. Rev. C* **67**, 064613 (2003).
- [35] W. Lin, X. Liu, M. R. D. Rodrigues, S. Kowalski, R. Wada, M. Huang, S. Zhang, Z. Chen, J. Wang, G. Q. Xiao, R. Han, Z. Jin, J. Liu, F. Shi, T. Keutgen, K. Hagel, M. Barbui, C. Bottosso, A. Bonasera, J. B. Natowitz, E. J. Kim, T. Materna, L. Qin, P. K. Sahu, K. J. Schmidt, S. Wuenschel, and H. Zheng, *Phys. Rev. C* **89**, 021601 (2014).
- [36] W. Lin, X. Liu, M. R. D. Rodrigues, S. Kowalski, R. Wada, M. Huang, S. Zhang, Z. Chen, J. Wang, G. Q. Xiao, R. Han, Z. Jin, J. Liu, P. Ren, F. Shi, T. Keutgen, K. Hagel, M. Barbui, C. Bottosso, A. Bonasera, J. B. Natowitz, T. Materna, L. Qin, P. K. Sahu, and H. Zheng, *Phys. Rev. C* **90**, 044603 (2014).
- [37] M. R. D. Rodrigues, W. Lin, X. Liu, M. Huang, S. Zhang, Z. Chen, J. Wang, R. Wada, S. Kowalski, T. Keutgen, K. Hagel, M. Barbui, C. Bottosso, A. Bonasera, J. B. Natowitz, T. Materna, L. Qin, P. K. Sahu, and K. J. Schmidt, *Phys. Rev. C* **88**, 034605 (2013).
- [38] X. Liu, W. Lin, R. Wada, M. Huang, P. Ren, Z. Chen, J. Wang, G. Xiao, S. Zhang, R. Han, J. Liu, F. Shi, M. Rodrigues, S. Kowalski, T. Keutgen, K. Hagel, M. Barbui, A. Bonasera, J. Natowitz, and H. Zheng, *Nuclear Physics A* **933**, 290 (2015).